Published in final edited form as:
J Biol Chem. 2007 October 5; 282(40): 29211–29221.

A Novel $Ca_V1.2$ N Terminus Expressed in Smooth Muscle Cells of Resistance Size Arteries Modifies Channel Regulation by Auxiliary Subunits[*,S]

Xiaoyang Cheng[‡,1], **Jianxi Liu**[§], **Maria Asuncion-Chin**[§], **Eva Blaskova**[‡], **John P. Bannister**[‡], **Alejandro M. Dopico**[§], and **Jonathan H. Jaggar**[‡,2]

‡ *Department of Physiology, University of Tennessee Health Science Center, Memphis, Tennessee 38163*

§ *Department of Pharmacology, University of Tennessee Health Science Center, Memphis, Tennessee 38163*

Abstract

Voltage-dependent L-type Ca^{2+} ($Ca_V1.2$) channels are the principal Ca^{2+} entry pathway in arterial myocytes. $Ca_V1.2$ channels regulate multiple vascular functions and are implicated in the pathogenesis of human disease, including hypertension. However, the molecular identity of $Ca_V1.2$ channels expressed in myocytes of myogenic arteries that regulate vascular pressure and blood flow is unknown. Here, we cloned $Ca_V1.2$ subunits from resistance size cerebral arteries and demonstrate that myocytes contain a novel, cysteine rich N terminus that is derived from exon 1 (termed "exon 1c"), which is located within *CACNA1C*, the $Ca_V1.2$ gene. Quantitative PCR revealed that exon 1c was predominant in arterial myocytes, but rare in cardiac myocytes, where exon 1a prevailed. When co-expressed with $\alpha_2\delta$ subunits, $Ca_V1.2$ channels containing the novel exon 1c-derived N terminus exhibited: 1) smaller whole cell current density, 2) more negative voltages of half activation ($V_{1/2,act}$) and half-inactivation ($V_{1/2,inact}$), and 3) reduced plasma membrane insertion, when compared with channels containing exon 1b. β_{1b} and β_{2a} subunits caused negative shifts in the $V_{1/2,act}$ and $V_{1/2,inact}$ of exon 1b-containing $Ca_V1.2\alpha_1/\alpha_2\delta$ currents that were larger than those in exon 1c-containing $Ca_V1.2\alpha_1/\alpha_2\delta$ currents. In contrast, β_3 similarly shifted $V_{1/2,act}$ and $V_{1/2,inact}$ of currents generated by exon 1b- and exon 1c-containing channels. β subunits isoform-dependent differences in current inactivation rates were also detected between N-terminal variants. Data indicate that through novel alternative splicing at exon 1, the $Ca_V1.2$ N terminus modifies regulation by auxiliary subunits. The novel exon 1c should generate distinct voltage-dependent Ca^{2+} entry in arterial myocytes, resulting in tissue-specific Ca^{2+} signaling.

Voltage-dependent L-type Ca^{2+} ($Ca_V1.2$)[3] channels are the primary Ca^{2+} entry pathway in arterial myocytes (1). Ca^{2+}entry through $Ca_V1.2$ channels regulates multiple physiological functions, including cell contractility and gene expression (2). In small resistance arteries and arterioles, $Ca_V1.2$ channels play a dominant role in myogenic tone development and blood pressure regulation (3,4). Smooth muscle-specific inactivation of the $Ca_V1.2$ gene

---

[*]This study was supported by grants from the National Institutes of Health (to J. H. J., HL67061 and HL77678; and A. M. D., AA11560 and HL77424) and the American Heart Association National Center (to J. H. J.).

[S]The on-line version of this article (available at http://www.jbc.org) contains supplemental Table S1.

[2] To whom correspondence should be addressed: Dept. of Physiology, University of Tennessee Health Science Center, 894 Union Ave., Memphis, TN 38163. Tel.: 901-448-1208; Fax: 901-448-7126; E-mail: jjaggar@physio1.utmem.edu.

[1]Recipient of a predoctoral fellowship from the Southeast Affiliate of the American Heart Association.

The nucleotide sequence(s) reported in this paper has been submitted to the Gen-Bank™/EBI Data Bank with accession number(s) DQ538522 and AY974797.

[3]The abbreviations used are: $Ca_V1.2$, voltage-dependent L-type Ca^{2+}; RACE, rapid amplification of cDNA ends; EGFP, enhanced green fluorescent protein; I-V, current-voltage.

(*CACNA1C*) dramatically reduces mean arterial blood pressure in mice, and arterial myocytes from hypertensive subjects exhibit increased L-type Ca^{2+} channel α_1 subunit expression (3, 5). Moreover, a variety of agents that selectively block L-type Ca^{2+} channels are widely used to treat hypertension because of their ability to reduce arterial myocyte contractility (6). However, despite the central role of $Ca_V1.2$ channels in cardiovascular physiology and pathology, the molecular identity of these channels in myocytes of small myogenic arteries that regulate blood pressure and flow is unknown.

In most tissues, native voltage-dependent Ca^{2+} channels consist of a pore-forming α_1 ($Ca_V1.2$) subunit and auxiliary β and $\alpha_2\delta$ subunits (7). $Ca_V1.2$ subunits contain the voltage sensor and several regulatory sites that determine the basic biophysical and pharmacological properties of the Ca^{2+} channel complex, whereas β and $\alpha_2\delta$ subunits regulate channel trafficking and gating kinetics (8). The human $Ca_V1.2$ gene can undergo alternative splicing at 19 out of 55 exons, leading to structural and functional $Ca_V1.2$ diversity (9). Vascular $Ca_V1.2$ subunits identified so far were cloned either from a whole organ, the rat aorta, or from a smooth muscle layer isolated by laser-capture microdissection from carotid or femoral arteries (10,11). In each of these studies, clones were derived from conduit vessels that do not develop myogenic tone or critically influence systemic or organ blood pressure (GenBank™ accession numbers: M59786, AY830711-AY830713, Z34811, and Z34812; Refs. 10 and 11). To better understand Ca^{2+}-dependent regulation of arterial smooth muscle physiology and to design more effective interventions for vascular pathologies associated with dysfunctional Ca^{2+} signaling, it is imperative to determine the molecular identity of $Ca_V1.2$ subunits expressed in myocytes of resistance size arteries. Conceivably, myocytes of myogenic arteries may express distinct subunit isoforms that confer tissue-specific physiology.

Here, we cloned full-length $Ca_V1.2$ subunits from small, myogenic cerebral arteries. Through the use of 5′-RACE, we found that $Ca_V1.2$ subunits expressed in myocytes of these arteries predominantly contain a novel, cysteine-rich N terminus encoded by alternative splicing of the $Ca_V1.2$ gene at exon 1. Electrophysiological studies indicate that the novel exon 1-derived N terminus modifies both $Ca_V1.2$ subunit current density and regulation by auxiliary subunits. Our study suggests that $Ca_V1.2$ exon 1, through alternative splicing, contributes to auxiliary subunit-mediated regulation of arterial myocyte voltage-dependent Ca^{2+} channels. Thus, splicing of the arterial myocyte $Ca_V1.2$ N terminus may contribute to tissue-specific Ca^{2+} entry and intracellular Ca^{2+} signaling.

EXPERIMENTAL PROCEDURES

Tissue Preparation

Procedures involving animals were approved by the Animal Care and Use Committee at the University of Tennessee. Sprague-Dawley rats (~250 g) were euthanized by peritoneal injection of sodium pentobarbital solution (150 mg/kg). For total RNA extraction, small (<200 μm) cerebral arteries, isolated cerebral artery myocytes, cardiac myocytes, aorta, heart, and brain, were prepared and placed immediately in TRIzol reagent (Invitrogen). Myocytes were enzymatically dissociated from rat cerebral arteries (~150 μm diameter) using a procedure similar to that previously described (12). Cardiac myocytes were prepared as previously described (13) and kindly provided by Dr. P. A. Hofmann in the Department of Physiology at UTHSC.

Reverse Transcription

First-strand cDNA was synthesized from ~3 μg of total RNA using oligo d(T) and reverse transcriptase (SuperScript™ III, Invitrogen).

Rapid Amplification of $Ca_V1.2$ 5′-End (5′-RACE) and Cloning of Full-length $Ca_V1.2$ Subunits

Primer sequences are provided in Table S1 of supplemental information. 5′-Ends of $Ca_V1.2$ subunits were generated using the BD SMART RACE cDNA amplification kit using gene-specific primer 1 (GSP1). Nested PCR was performed using GSP2 and UPM primers. Nested PCR products were purified and ligated into the pGEM-T easy vector (Promega) and transformed in JM109 cells. Plasmids containing inserts were sequenced using a T7 promoter primer (Promega), which revealed two different $Ca_V1.2$ 5′-end sequences. Full-length $Ca_V1.2$ subunits were amplified from cerebral artery cDNA with primers designed to recognize the two different 5′-ends (sense 6 and antisense 4 for the exon 1b-containing subunit, termed $Ca_V1.2$e1b, and sense 5 and antisense 4 for the exon 1c-containing subunit, termed $Ca_V1.2$e1c) using the Expand Long Template PCR System (Roche Applied Science). Antisense 4 was designed according to the highly conserved 3′-untranslated region of known $Ca_V1.2$ sequences (GenBank™ accession number: rat brain, M67515, M67516; rat aorta, M59786). PCR products were ligated into pGEM-T easy vector (Promega) for selection. Plasmids containing DNA inserts were sequenced at the University of Tennessee Molecular Resource Center.

Polymerase Chain Reaction

To identify the presence of exon 1a, exon 1b, exon 1c, β_{1b}, β_{2a}, and β_3, two consecutive rounds of PCR were performed. The first PCR round was 20 cycles, and the second PCR round was 40 cycles. PCR reactions were started with a 2-min initial denaturation at 94 °C, then thermocycled at 94 °C for 30 s, 56 °C for 30 s, and 72 °C for 30 s in the first round of PCR, or 60 s in the second round of PCR, followed by 72 °C for 3 or 5 min. PCR products were separated in 2% agarose gels. Primer pairs of the first round PCR were: exon 1c-176S1 and exon2-A1 for $Ca_V1.2$e1c; exon 1b-97S1 and exon 2-A1 for $Ca_V1.2$e1b; actin-2794S1 and actin-3337A1 for β actin. Primer pairs of the second round PCR were: exon 1c-201S2 and exon 1c-382A2 for $Ca_V1.2$e1c; exon 1b-137S2 and exon 1b-287A2 for $Ca_V1.2$e1b; actin-2901S2 and actin-3037A2 for β actin. A similar procedure was used to identify $Ca_V\beta$ subunits in arterial myocytes. Primers used for amplification of β_{1b} (X61394, Ref. 14), β_{2a} (M80545, Ref. 15), and β_3 (M88751, Ref. 16) are listed in supplemental Table S1. pGW-β_{1b}, pcDNA3-β_{2a}, and pcDNA3-β_3 were used as positive controls.

Identification of Exons 1a, 1b, 1c, and $Ca_V\beta$ Subunits in Rat Cerebral Artery Myocytes and Cardiac Myocytes

Individual arterial myocytes or cardiac myocytes were visualized using an inverted microscope (Nikon, TS100) and aspirated individually into a small glass pipette, as described previously (17). Reverse transcription was performed with 2–10 myocytes using SuperScript III reverse transcriptase (Invitrogen). Two consecutive PCR rounds were performed to identify the presence of exon 1a, 1b, 1c, β_{1b}, β_{2a}, and β_3. PCR products were verified by sequencing.

Quantitative Real Time PCR

$Ca_V1.2$ cDNA was synthesized from 2–10 rat arterial myocytes that were collected as described above. One initial 20-cycle round of PCR was performed, and the PCR products were used as templates for real-time PCR using the QuantiTect SYBR Green PCR kit (Qiagen). The primer pairs used in identification experiments were also used for real time PCR of exon 1b and 1c, except that Exon 1c-201S2 was replaced with Exon 1c-230S2. For exon 1a, Exon 1a-134S1 and Exon 2-A1 were used in initial PCR, and Exon 1a-188S2 and Exon 1a-340A2 were used in real time PCR. Amplification efficiency was evaluated from the slope of the regression curve obtained with several dilutions of cardiac cDNA, and the specificity of primers was tested by melting curve analysis. A mean amplification efficiency of 1.92 was used for calculating the relative percentage of exon 1a, 1b, and 1c mRNA in cerebral artery myocytes and cardiac myocytes.

Construction of Expression Vectors for L-type Ca^{2+} Channel α_1 Subunits

For electrophysiological characterization, full length $Ca_V1.2e1b$ and $Ca_V1.2e1c$ were subcloned from the pGEM-T easy vector into the pIRES-hrGFP II vector (Stratagene) using NotI and T4 ligase for expression. EcoRV was used to examine the ligation direction. Constructs with correct nucleotide sequences were transformed into $DH_{5\alpha}$ cells, purified with the HiSpeed plasmid maxi kit (Qiagen), and stored at −20 °C. For generation of EGFP-tagged $Ca_V1.2$, $Ca_V1.2e1b$ and $Ca_V1.2e1c$ coding sequences were amplified from pIRES-$Ca_V1.2e1b$-hrGFP II and pIRES-$Ca_V1.2e1c$-hrGFP II, respectively, using PfuUltra II fusion HS DNA polymerase (Stratagene) with the following primers: forward, CACCGTCGACCTGCAGATATCCATCACACTGG; reverse, CACCCCGCGGCCAGGTTGCTGACATAGGACC. cDNAs were purified and ligated into pEGFP-N3 vector using SalI and SacII. The reading frames of pEGFP-$Ca_V1.2e1c$-N3 and pEGFP-$Ca_V1.2e1b$-N3 vectors were confirmed by sequence analysis.

Cell Culture and Transient Transfection

COS-1 and HEK 293 cells (ATCC) were maintained in DMEM-F12 (Cellgro) supplemented with 10% FBS under standard tissue culture conditions (5% CO_2, 37 °C). Endogenous $Ca_V1.2$ subunits are not present in significant amounts in COS-1 and HEK 293 cells (18,19). Cells for transfection were grown in 35-mm Petri dishes and transiently transfected using FuGENE6 (Roche Applied Science). COS-1 cells were used for patch clamp electrophysiology experiments following transfection with different combinations of pIRES-$Ca_V1.2e1c$-hrGFP II, pIRES-$Ca_V1.2e1b$-hrGFP II, pGW-β_{1b}, pcDNA3-β_{2a}, pcDNA3-β_3, and pcDNA3-$\alpha_2\delta$-1 (1 μg of each). HEK 293 cells were used for channel localization measurements because plasma membrane fluorescence originating from EGFP-tagged $Ca_V1.2$ channels could be more effectively differentiated from that in intracellular compartments than with COS-1 cells. HEK 293 cells were transfected with different combinations of pEGFP-$Ca_V1.2e1b$-N3 or pEGFP-$Ca_V1.2e1c$-N3 (0.5 μg) and pcDNA3-$\alpha_2\delta$-1 and pGW-β_{1b} (1 μg of each). Cells were maintained in a 95% O_2/5% CO_2 atmosphere at 37 °C and used for electrophysiological and fluorescence experiments between 36 and 72 h after transfection. pGW-β_{1b} was kindly provided by Dr. Henry Colecraft (Johns Hopkins University School of Medicine), pcDNA3-β_{2a} by Dr. Timothy J. Kamp (University of Wisconsin Medical School), and pcDNA3-β_3 and pcDNA3-$\alpha_2\delta$-1 by Dr. Diane Lipscombe (Brown University).

Patch Clamp Electrophysiology

Whole cell patch clamp recordings were acquired at room temperature using an Axo-patch 200B amplifier (Axon Instruments, Foster City, CA) and pCLAMP 8.2 or 9.2. Borosilicate glass electrodes of resistance 1–3 MΩ were filled with pipette solution containing (in mmol/liter): for COS-1 cells, Cs-$MeSO_3$ 135, CsCl 5, EGTA 5, MgATP 4, Na_2GTP 0.25, HEPES 10, and glucose 10 (pH 7.2, adjusted with CsOH); for arterial myocytes, CsCl 140, EGTA 5, MgATP 4, HEPES 10, and glucose 10 (pH 7.2, with CsOH). The extra-cellular bath solution contained (in mmol/liter): for COS-1 cells, NaCl 80, TEACl 60, $MgCl_2$ 1, HEPES 10, $BaCl_2$ 5, and glucose 10 (pH 7.4, adjusted with NaOH), for myocytes, TEACl 140, $MgCl_2$ 1, HEPES 10, $BaCl_2$ 20, and glucose 10 (pH 7.4, adjusted with TEAOH). Myocyte voltage-dependent Ba^{2+} currents were isolated by subtracting Cd^{2+} (250 μM)-insensitive currents from whole cell currents. Solutions were ~300 mOsm, as measured using a Vapor Pressure Osmometer. Isolated cells that were not visibly attached to neighboring cells were used for patch clamp. Cell capacitance was measured by applying a 5-mV test pulse and correcting the capacitance transients with series resistance compensation. For measurement of current-voltage (I-V) relationships, cells were clamped at −80 mV and whole cell currents were evoked every 5 s by 300-ms step depolarizations to between −60 and +60 mV in 10-mV increments. Steady-state inactivation was measured every 15 s by providing 1-s conditioning pulses to between −80 and

+60 mV (+30 mV for $\alpha_1/\beta_3/\alpha_2\delta$) in 10-mV increments before a 200-ms test pulse to 0 mV. A 15-ms return to −80 mV was applied after the conditioning pulse and prior to the test pulse. Tail currents were generated by repolarization to −80 mV after a series of 20-ms test pulses to between −60 mV and +60 mV in 10-mV increments. Whole cell currents were filtered at 1–2 kHz and digitized at 4 – 10 kHz. P/4 protocols were used to subtract leak and capacitive transients. Steady-state inactivation curves and tail currents were fit with the Boltzmann function in Equation 1,

$$I/I_{max} = R_{in} + (R_{max} - R_{in})/(1 + \exp((V - V_{1/2})/k)) \quad \text{(Eq. 1)}$$

where I/I_{max} is the normalized peak current, V is the conditioning pre-pulse voltage, $V_{1/2}$ is the voltage for half-inactivation for steady-state inactivation or half-activation for tail currents, k is the slope factor, R_{in} is the proportion of non-inactivating current, R_{max} is the maximal current. Inactivation time constants (τ) were obtained using Equation 2,

$$I_t = I_{fast} \cdot e^{-t/\tau fast} + I_{slow} \times e^{-t/\tau fast} + I_\theta \quad \text{(Eq. 2)}$$

where I_t is the inward current at time t, and I_θ is the residual current.

Confocal Microscopy

HEK 293 cells transfected with EGFP-tagged $Ca_V1.2$ α_1 subunits and either $\alpha_2\delta$ or $\alpha_2\delta + \beta_{1b}$ were visualized using a Zeiss LSM 5 Pascal laser-scanning confocal microscope. EGFP was excited using 488 nm light, and >510 nm light was collected. Analysis methodology similar to that previously described was used to calculate plasma membrane localized fluorescence originating from EGFP-tagged $Ca_V1.2$ $\alpha1$ subunits containing either the exon 1b or exon 1c-derived N terminus (20). Briefly, membrane boundaries were established by visualizing DIC images using a membrane thickness of 0.55 μm. Using these boundaries, membrane localized fluorescence was calculated from background subtracted fluorescence images. For each cell, total membrane-localized fluorescence was calculated by subtracting cytoplasmic fluorescence from total cellular fluorescence. Total membrane fluorescence was then divided by membrane area (in μm^2) to establish average membrane fluorescence. Image analysis was performed using Image J software (NIH).

Data Analysis

Electrophysiological data were analyzed using Clampfit 8.2 and 9.2 and Origin 7.5. Values are expressed as means ± S.E. Student's *t*-tests were used for comparing paired or unpaired data, and one-way analysis of variance and Student-Newman-Keuls or Dunn posthoc tests were used for comparing multiple data sets. $p < 0.05$ was considered significant.

RESULTS

To identify voltage-dependent Ca^{2+} channels present in myocytes of small cerebral arteries, we first measured currents in these cells using patch clamp electrophysiology. Fig. 1*A* illustrates Cd^{2+} (250 μM)-sensitive, voltage-dependent Ba^{2+} currents characteristic of $Ca_V1.2$ that were recorded in cerebral artery myocytes (Fig. 1*A*). To proceed to clone full-length $Ca_V1.2$ subunits from small cerebral artery myocytes using PCR, we first sought to identify the $Ca_V1.2$ 5′-end sequence(s) expressed in these cells. Two different $Ca_V1.2$ N termini have previously been described (21). Exon 1a encodes the $Ca_V1.2$ subunit N terminus found in whole heart (22) and whole aorta(10), and exon 1b (also referred to as exon 1) encodes the N terminus detected in whole brain (23), lung (24), and jejunum $Ca_V1.2$ subunits (25). $Ca_V1.2$ 5′-ends expressed in resistance size (<200 μm diameter) cerebral arteries were amplified using 5′-RACE and ligated into pGEM-T easy vector (Fig. 1*B*). Sequencing analysis of 11 plasmids

revealed two different $Ca_V1.2$ subunit 5′-ends (Fig. 1*C*). One did not match any sequence previously described, but was mapped within *CACNA1C* of the rat genome. The second sequence was identical to the previously described exon 1b. Exon 1a was not detected by 5′-RACE. According to their relative location within the rat genome, the sequence previously described in brain, lung and jejunum (exon 1) was termed "exon 1b", and the novel 5′-end was termed "exon 1c" (Fig. 1, *C* and *D*). Exon 1c is responsible for encoding a 9 amino acid peptide, and substituting glycine at the exon 1/2 junction for cysteine (Fig. 1*E*). This substitution generates the cysteine-rich N-terminal sequence: MLCCALDCAC.

To examine whether exon 1b and 1c were expressed in arterial myocytes, RT-PCR was performed using small groups (~10) of manually selected cerebral artery myocytes (see "Experimental Procedures"). Critically, this methodology avoids contamination from other vascular wall cell types, including fibroblasts and perivascular neurons that express voltage-dependent Ca^{2+} channel subunits, including $Ca_V1.2$ (26,27). Both exons 1b and 1c were detected in cerebral artery myocytes (Fig. 2*A*). Next, to examine whether exon 1c exhibits arterial myocyte-specific expression, real-time PCR was performed on dissociated arterial and cardiac myocytes. Data indicated that exon 1c was predominant (~96%) in cerebral artery myocytes (Fig. 2*B*) Exons 1a, 1b, and 1c were all detected in cardiac myocytes, with exon 1a prevalent (~82%) and exons 1b and 1c each less than 15% of total message (Fig. 2*B*). Together, these data indicate that in the cardiovascular system, exon 1c message is predominant in arterial myocytes and scarce in cardiac myocytes.

Using 5′-end primers specific to either exon 1b or exon 1c, full length $Ca_V1.2$ cDNAs were amplified (forward primers: sense6 for exon 1b, sense5 for exon 1c; reverse primer: anti-sense4), and termed "$Ca_V1.2e1b$" (GenBank™ accession number: DQ538522) and "$Ca_V1.2e1c$" (AY974797), according to their exon 1 sequences (Fig. 3, *A* and *B*). The coding region of the $Ca_V1.2e1c$ subunit contains 6,477 nucleotides (including the stop codon) and encodes a 2,158-amino acid protein, whereas $Ca_V1.2e1b$ contains 6,498 nucleotides and encodes a 2,165-amino acid protein. $Ca_V1.2e1b$ and $Ca_V1.2e1c$ are identical except for their exon 1-derived N termini. Each variant contains exon 8, 9 + 9a, 21, and 32 + 33, consistent with $Ca_V1.2$ subunits identified in large, conduit arteries (11, 28).

To investigate whether exon 1 splicing imprints a distinct functionality to the voltage-dependent Ca^{2+} channel in arterial myocytes, $Ca_V1.2e1b$ or $Ca_V1.2e1c$ were subcloned into pIRES-hrGFP II vector and transfected in COS-1 cells for electrophysiological characterization. Voltage-dependent Ba^{2+} currents (I_{Ba}) were absent in non-transfected cells (data not shown). When co-expressed with $\alpha_2\delta$, maximal I_{Ba} for both $Ca_V1.2e1b$ and $Ca_V1.2e1c$ occurred at +10 mV (Fig. 4, *A* and *B*, Table 1). However, the mean peak current density of $Ca_V1.2e1b/\alpha_2\delta$ currents was ~2-fold larger than for $Ca_V1.2e1c/\alpha_2\delta$ currents (Fig. 4, *B* and *C*, Table 1). Voltages of steady-state half-inactivation ($V_{1/2,inact}$) and half-activation ($V_{1/2,act}$) of $Ca_V1.2e1c/\alpha_2\delta$ currents were also ~7 and ~5 mV more negative than those of $Ca_V1.2e1b/\alpha_2\delta$ currents, respectively (Fig. 4, *B* and *C*, Table 1). In contrast, inactivation rate constants of $Ca_V1.2e1c/\alpha_2\delta$ and $Ca_V1.2e1b/\alpha_2\delta$ currents were similar (Fig. 4*D*). These data indicate that when co-expressed with $\alpha_2\delta$, the novel exon 1c-derived $Ca_V1.2$ N terminus attenuates membrane current density and induces a negative shift in both $V_{1/2,act}$ and $V_{1/2,inact}$, when compared with currents mediated by channels containing the $Ca_V1.2$ exon 1b-derived N terminus.

Ca^{2+} channel β subunits regulate $Ca_V1.2$ channel voltage-dependence in an isoform-specific manner. For example, β_{2a} causes slow inactivation when compared with other β subunits (29,30). Expression of β subunits has been investigated in whole aorta (31), but not in myocytes of small, resistance size arteries. Here, we investigated the transcription of three different β subunits. Using RT-PCR, we studied β_{1b} and β_{2a}, which are membrane associated, and β_3,

which is cytosolic (8). β_{1b} and β_3 were detected in dissociated cerebral artery myocytes, whole aorta, and brain (Fig. 5, *A* and *C*). Although β_{2a} was present in whole cerebral artery, aorta, and brain, message was not detected in isolated cerebral artery myocytes (Fig. 5*B*). Data suggest that β_{2a} expression in arterial myocytes is either very low, or that β_{2a} is expressed predom inantly in cerebral artery wall cell types other than myocytes (*e.g.* neurons).

We sought to explore the functional effects of N-terminal splicing on β subunit regulation of $Ca_V1.2$. Although β_{2a} was not detected in cerebral artery myocytes, β_{2a} may be expressed in other cell types that contain the exon 1c $Ca_V1.2$ variant. Thus, β_{1b}, β_{2a}, or β_3 regulation of $Ca_V1.2e1b$ and $Ca_V1.2e1c$ currents was investigated. Fig. 6 illustrates raw current traces for $Ca_V1.2e1c$ and mean data obtained with $Ca_V1.2e1b$ and $Ca_V1.2e1c$ when co-expressed with $\alpha_2\delta$ and each β subunit isoform. Co-expression of β_{1b}, β_{2a}, or β_3 with $\alpha_2\delta$ increased $Ca_V1.2e1b$ and $Ca_V1.2e1c$ current density and eliminated the current density difference that occurred between $Ca_V1.2e1b/\alpha_2\delta$ and $Ca_V1.2e1c/\alpha_2\delta$ (Table 1). β subunits also shifted I-V relationships further to the left, with maximal I_{Ba} occurring at ~0 mV. However, β_{1b} shifted the $V_{1/2,inact}$ of $Ca_V1.2e1b/\alpha_2\delta$ currents by ~−16 mV, compared with only an ~−5 mV shift in the $V_{1/2,inact}$ of $Ca_V1.2e1c/\alpha_2\delta$ currents. At 0 and +10 mV, the slow component of inactivation (τ_{slow}) decayed more rapidly for $Ca_V1.2e1b/\alpha_2\delta/\beta_{1b}$ currents than for $Ca_V1.2e1c/\alpha_2\delta/\beta_{1b}$ currents, whereas the fast component (τ_{fast}) was similar (Fig. 6*G*). β_{2a} caused an ~−12 mV shift in the $V_{1/2,inact}$ of $Ca_V1.2e1b/\alpha_2\delta$ currents, but had no effect on the $V_{1/2,inact}$ of $Ca_V1.2e1c/\alpha_2\delta$ currents. Current inactivation rate was similar for $Ca_V1.2e1b/\alpha_2\delta/\beta_{2a}$ and $Ca_V1.2e1c/\alpha_2\delta/\beta_{2a}$ (Fig. 6*H*). β_3 similarly shifted the $V_{1/2,inact}$ of $Ca_V1.2e1b/\alpha_2\delta$ and $Ca_V1.2e1c/\alpha_2\delta$ currents; by −14 and −10 mV, respectively (Table 1). In contrast to effects with β_{1b}, between −10 and +10 mV τ_{slow} decayed more slowly for $Ca_V1.2e1b/\alpha_2\delta/\beta_3$ currents than for $Ca_V1.2e1c/\alpha_2\delta/\beta_3$ currents, although τ_{fast} was similar (Fig. 6*I*).

A similar pattern was observed with β subunit-mediated regulation of voltage-dependent activation. β_{1b} and β_{2a} caused a larger negative shift in the $V_{1/2,act}$ of $Ca_V1.2e1b/\alpha_2\delta$ currents than in $Ca_V1.2e1c/\alpha_2\delta$ currents (Table 1). In contrast, β_3 similarly shifted the $V_{1/2,act}$ of $Ca_V1.2/\alpha_2\delta$ currents, regardless of the exon 1 splice variant. Collectively, these data indicate that alternative splicing of the exon 1-derived $Ca_V1.2$ N terminus modifies regulation by β subunits and suggest that modifications in current phenotype are specific to particular β subunit isoforms.

To further study membrane insertion of $Ca_V1.2$ containing exon 1b or 1c, vectors that express EGFP fused to the C terminus of $Ca_V1.2e1b$ or $Ca_V1.2e1c$ channels were constructed. Membrane localization of expressed channels was studied using confocal microscopy. In agreement with current density measurements, when co-expressed with $\alpha_2\delta$ membrane fluorescence intensity of $Ca_V1.2e1b$-EGFP channels was higher than for $Ca_V1.2e1c$-EGFP channels (Fig. 7, *A* and *B*). Co-expression of β_{1b} further increased $Ca_V1.2e1b$-EGFP and $Ca_V1.2e1c$-EGFP fluorescence intensity and normalized the difference between the N-terminal isoforms that occurred when each was co-expressed with only $\alpha_2\delta$ (Fig. 7, *A* and *B*). These data indicate that alternative splicing between exon 1b and 1c modifies $Ca_V1.2$ channel membrane insertion in the presence of $\alpha_2\delta$, and this difference can be normalized by co-expression of a β subunit.

DISCUSSION

In the present study, we have for the first time cloned full-length $Ca_V1.2$ subunits expressed in small, resistance size, arteries and discovered a novel 5′-end sequence generated by alternative splicing at exon 1. Termed “exon 1c”, this sequence encodes a unique N terminus in which 4 out of 9 amino acids are cysteine residues. Quantitative PCR indicates that the vast majority (~96%) of $Ca_V1.2$ mRNA in isolated cerebral artery myocytes contains exon 1c, with

the residual proportion containing exon 1b, the previously reported "brain" $Ca_V1.2$ subunit exon 1 (23). In contrast, exon 1a was entirely absent in cerebral artery myocytes, as determined by both 5′-RACE and quantitative PCR. While exons 1a, 1b, and 1c were all detected in isolated cardiac myocytes, exon 1a was prevalent and the relative expression of exon 1c (~13%) was much lower than in arterial myocytes. Therefore, in the cardiovascular system, exon 1c is likely to be predominant in arterial myocyte $Ca_V1.2$ subunits, whereas exon 1a would be prevalent in cardiac myocyte $Ca_V1.2$. Two different promoters drive the expression of $Ca_V1.2$ channels containing exon 1a- and 1b-derived N termini in heart and smooth muscle, which may explain their different expression profiles (32,33). However, promoters which drive exon 1c expression are unclear.

Electrophysiological and imaging studies revealed that when co-expressed with $\alpha_2\delta$ subunits, current density generated by $Ca_V1.2e1b$ was significantly greater than for $Ca_V1.2e1c$. In addition, when co-expressed with $\alpha_2\delta$, membrane fluorescence intensity of EGFP-tagged $Ca_V1.2e1b$ channels was higher than that of $Ca_V1.2e1c$ channels. Four genes encode $\alpha_2\delta$ subunits, and $\alpha_2\delta$-1, the isoform used here, increases $Ca_V1.2$ membrane insertion and alters channel inactivation (34). α_2 is an extracellular domain that associates with the plasma membrane through a disulfide-bond with the membrane-spanning δ domain (8). Glycosylation of the α_2 domain is essential for $\alpha_2\delta$-mediated membrane insertion of $Ca_V1.2$ subunits (35). In contrast, δ mimics the effects of full-length $\alpha_2\delta$ on channel kinetics (36). Each N terminus might interact differently with $\alpha_2\delta$, leading to the observed differences between $Ca_V1.2e1b$ and $Ca_V1.2e1c$ channels. Alternatively, differences in $Ca_V1.2e1b$ and $Ca_V1.2e1c$ channels might be interpreted as different conformational channel states controlled by the different N termini of $Ca_V1.2$ subunits, which only become evident in the presence of $\alpha_2\delta$ subunits. Regardless of the molecular underpinnings, our study indicates that alternative splicing of exon 1 alters both channel voltage sensitivity and current density.

β subunits regulate $Ca_V1.2$ properties by binding to the Alpha Interaction Domain (AID) in the I-II linker (37). However, because a single amino acid mutation in the AID does not eliminate β-subunit-mediated modulation of $Ca_V1.2$ subunits, additional interaction sites between α_1 and β subunits likely exist (38). Our data revealed that β_{1b} and β_3 were present in isolated cerebral artery myocytes, whereas β_{2a} was found only in intact cerebral arteries. Only one rat β_{2a} sequence has been described, but multiple splice variants of human β_{2a} exist (NCBI search, November 6, 2006) (39,40). The primers used in our study to detect β_{2a} message recognize a rat β_{2a} sequence that corresponds to a highly conserved region in all five human splice variants. Thus, it appears to be unlikely that β_{2a} splice variants not recognized by the primers used here exist in rat arterial smooth muscle. These data underscore the need for caution when extrapolating RT-PCR data obtained using whole arterial cDNA to message levels present in myocytes. Future studies will determine whether exon 1c is also predominant in myocytes of other arteries, or is a specific cerebral artery splice variant.

β_3 is a cytosolic-localized protein, whereas β_{1b} and β_{2a} associate with the plasma membrane through either an acidic motif within the C terminus or palmitoylation sites in the N terminus, respectively (41,42). When compared with currents obtained with $\alpha_2\delta$ alone, all three β subunits elevated current density, with a greater increase seen in $Ca_V1.2$ channels containing exon 1c than in channels containing exon 1b, which abolished the current density difference between $Ca_V1.2e1b/\alpha_2\delta$ and $Ca_V1.2e1c/\alpha_2\delta$ currents. β_{1b} also normalized the difference in membrane fluorescence intensity between $Ca_V1.2e1b/\alpha_2\delta$ and $Ca_V1.2e1c/\alpha_2\delta$ channels. β_3 caused similar shifts in both the $V_{1/2,inact}$ and $V_{1/2,act}$ of $Ca_V1.2e1b/\alpha_2\delta$ and $Ca_V1.2e1c/\alpha_2\delta$ currents, while β_{1b} and β_{2a} caused larger negative shifts in $Ca_V1.2e1b/\alpha_2\delta$ currents than in $Ca_V1.2e1c/\alpha_2\delta$ currents. When co-expressed with either β_{1b} or β_3, the decay of $Ca_V1.2/\alpha_2\delta$ currents containing e1b or e1c was best fit by a bi-exponential function. Substitution of e1b for e1c decelerated the slow decay component of $Ca_V1.2/\alpha_2\delta/\beta_{1b}$ currents. In contrast, e1c accelerated the slow

decay of $Ca_V1.2/\alpha_2\delta/\beta_3$ currents, when compared with e1b. The rates of decay of $Ca_V1.2/\alpha_2\delta$ or $Ca_V1.2/\alpha_2\delta/\beta_{2a}$ currents were best fit with a single exponential function and were similar in $Ca_V1.2$ currents containing either the exon 1b or exon 1c-derived N terminus. Collectively, these data suggest that the $Ca_V1.2$ N terminus modifies β subunit-mediated channel regulation. These findings also indicate that in the presence of a β subunit, not only is the rate of slow inactivation modulated by splicing of the N terminus, but also that kinetic alterations depend on the β subunit isoform involved. In contrast, exon 1b or 1c-derived N termini do not appear to significantly alter fast inactivation.

$Ca_V1.2e1c$ contains 4 cysteine residues, which are putative palmitoylation sites. One function of palmitoylation is to aid protein targeting to lipid rafts in the plasma membrane (43). Conceivably, different local lipid microenvironments may explain distinctions between $Ca_V1.2e1b$ and $Ca_V1.2e1c$ currents. It is also possible that the cysteine-rich N terminus regulates $Ca_V1.2e1c$ channels by interacting with other cellular molecules and regulatory proteins, since cysteine-cysteine interactions that occur through disulfide bridging can alter channel folding and protein-protein interactions (44,45). Immobilization of the $Ca_V1.2$ N terminus also inhibits both voltage- and Ca^{2+}-dependent inactivation (19). Although not defined here, our results pave the way for future studies to determine the full range of mechanisms by which exon 1b and 1c encoded N termini regulate $Ca_V1.2$ channel phenotypes.

In native arterial myocytes, the current phenotype produced by channels containing $Ca_V1.2$ subunits and thus, voltage-dependent Ca^{2+} influx, is the result of an orchestration of factors. A majority of $Ca_V1.2$ channels containing an N terminus derived from exon 1c rather than exon 1b could modify voltage-dependent Ca^{2+} influx through several mechanisms. First, $Ca_V1.2e1c/\alpha_2\delta$ current density was smaller than for $Ca_V1.2e1b/\alpha_2\delta$. Second, $Ca_V1.2e1c/\alpha_2\delta$ currents inactivated at more negative voltages than $Ca_V1.2e1b/\alpha_2\delta$ currents. Third, when co-expressed with $\alpha_2\delta$, less $Ca_V1.2e1c$ channels localized to the plasma membrane than did $Ca_V1.2e1b$ channels. Collectively, these exon 1c-derived effects would reduce voltage-dependent Ca^{2+} influx in arterial myocytes. Arterial myocytes do not generate action potentials, but undergo steady-state changes in membrane potential. In arteries at physiological pressures, myocyte membrane potential is between ~−60 and −40 mV (46). Thus, arterial myocytes maintain relatively depolarized potentials when compared with many other cell types, particularly those that generate action potentials. A predominance of $Ca_V1.2$ channels containing exon 1c may serve to limit Ca^{2+} influx under the steady depolarized potentials that occur in arterial myocytes. Because arterial myocyte membrane potential changes steadily rather than rapidly (as in the case of action potentials), differences in inactivation rates between $Ca_V1.2e1b/\alpha_2\delta/\beta$ and $Ca_V1.2e1c/\alpha_2\delta/\beta$ channels would presumably have a smaller influence on Ca^{2+} influx than the exon 1c-induced alterations in current density, steady-state inactivation, and membrane insertion. Because $Ca_V1.2$ $\alpha1$ sub-units undergo splicing at 19 out of 55 exons, and some of these variants have also been described to modify channel electro-physiological properties, it is premature to provide a detailed comparison of properties of the splice variants described here and what is likely to be a heterogeneous $Ca_V1.2$ splice variant population in myocytes (9). Furthermore, auxiliary subunit expression in arterial myocytes, which would modify $Ca_V1.2$ currents, is also unclear. Even though we detected β_{1b} and β_3 message in arterial myocytes, it is uncertain which other β subunit isoforms are expressed, the relative proportions of each isoform, the relative amount of β to $\alpha_2\delta$ subunits, the relative proportions of each auxiliary subunit to α_1 subunits, and whether β and $\alpha_2\delta$ subunit isoforms exhibit defined cellular localization that could specifically modify the properties of α_1 subunits containing exon 1b- or 1c-derived N termini. The electrophysiological properties of arterial myocyte $Ca_V1.2$ currents result from the combination of these additional, multiple factors. Nevertheless, our data indicate that electrophysiological properties of $Ca_V1.2$ currents are modified by splicing of the $Ca_V1.2$ $\alpha1$ subunit N terminus. Although β subunits normalized the isoform specific effects of $\alpha_2\delta$ on $Ca_V1.2e1b$ and$Ca_V1.2e1c$ channels in an overexpression system, it remains

to be determined whether this occurs in arterial myocytes in physiology and disease. Given that alternative splicing of $Ca_V1.2$ subunits has been observed in disease (11,47), and that $Ca_V1.2$ subunit expression is up-regulated in arterial myocytes of hypertensive animals (5), modifications in exon 1 splicing could occur during vascular disease and may contribute to increased $Ca_V1.2$ expression in hypertension.

In the human genome, sequences highly homologous to exon 1a and 1b are present in the $Ca_V1.2$ gene, yet a sequence identical to 1c is not found. A sequence that shares high homology with the 5′-untranslated region upstream of exon 1c is present in the human genome (p13.33 of chromosome 12), raising the possibility that $Ca_V1.2$ channels in human arterial myocytes contain an N terminus different to that described in human jejunum (25). Future studies will be required to identify human $Ca_V1.2$ $\alpha 1$ subunit exon 1 splice variants in arterial myocytes and other cell types.

In summary, we have established that $Ca_V1.2$ subunits which are expressed in myocytes of small, resistance size, cerebral arteries contain a novel exon 1c-derived splice variant that alters current regulation by auxiliary subunits. Considering the critical importance of $Ca_V1.2$ channels in the regulation of blood pressure and flow, and their role in vascular pathologies, including hypertension (5), exon 1c likely contributes to vascular specific Ca^{2+} signaling and Ca^{2+}-dependent physiology.

Supplementary Material

Refer to Web version on PubMed Central for supplementary material.

Acknowledgements

We thank Dr. Steven J. Tavalin for helpful discussions on the manuscript.

References

1. Gollasch M, Nelson MT. Kidney Blood Press Res 2000;20:355–371. [PubMed: 9453447]
2. Berridge MJ, Lipp P, Bootman MD. Nat Rev Mol Cell Biol 2000;1:11–21. [PubMed: 11413485]
3. Moosmang S, Schulla V, Welling A, Feil R, Feil S, Wegener JW, Hofmann F, Klugbauer N. EMBO J 2003;22:6027–6034. [PubMed: 14609949]
4. Nelson MT, Patlak JB, Worley JF, Standen NB. Am J Physiol 1990;259:C3–18. [PubMed: 2164782]
5. Sonkusare S, Palade PT, Marsh JD, Telemaque S, Pesic A, Rusch NJ. Vascul Pharmacol 2006;44:131–142. [PubMed: 16427812]
6. Triggle DJ. Curr Pharm Des 2006;12:443–457. [PubMed: 16472138]
7. Catterall WA, Perez-Reyes E, Snutch TP, Striessnig J. Pharmacol Rev 2005;57:411–425. [PubMed: 16382099]
8. Arikkath J, Campbell KP. Curr Opin Neurobiol 2003;13:298–307. [PubMed: 12850214]
9. Tang ZZ, Liang MC, Lu S, Yu D, Yu CY, Yue DT, Soong TW. J Biol Chem 2004;279:44335–44343. [PubMed: 15299022]
10. Koch WJ, Ellinor PT, Schwartz A. J Biol Chem 1990;265:17786–17791. [PubMed: 2170396]
11. Tiwari S, Zhang Y, Heller J, Abernethy DR, Soldatov NM. Proc Natl Acad Sci U S A. 2006
12. Jaggar JH. Am J Physiol 2001;281:C439–448.
13. Liu Q, Hofmann PA. Am J Physiol Heart Circ Physiol 2003;285:H97–103. [PubMed: 12649078]
14. Pragnell M, Sakamoto J, Jay SD, Campbell KP. FEBS Lett 1991;291:253–258. [PubMed: 1657644]
15. Perez-Reyes E, Castellano A, Kim HS, Bertrand P, Baggstrom E, Lacerda AE, Wei XY, Birnbaumer L. J Biol Chem 1992;267:1792–1797. [PubMed: 1370480]
16. Castellano A, Wei X, Birnbaumer L, Perez-Reyes E. J Biol Chem 1993;268:3450–3455. [PubMed: 7679112]

17. Jaggar JH, Li A, Parfenova H, Liu J, Umstot ES, Dopico AM, Leffler CW. Circ Res 2005;97:805–812. [PubMed: 16166559]
18. Meir A, Bell DC, Stephens GJ, Page KM, Dolphin AC. Biophys J 2000;79:731–746. [PubMed: 10920007]
19. Kobrinsky E, Tiwari S, Maltsev VA, Harry JB, Lakatta E, Abernethy DR, Soldatov NM. J Biol Chem 2005;280:12474–12485. [PubMed: 15671035]
20. Pietrzykowski AZ, Martin GE, Puig SI, Knott TK, Lemos JR, Treistman SN. J Neurosci 2004;24:8322–8332. [PubMed: 15385615]
21. Liao P, Yong TF, Liang MC, Yue DT, Soong TW. Cardiovasc Res 2005;68:197–203. [PubMed: 16051206]
22. Mikami A, Imoto K, Tanabe T, Niidome T, Mori Y, Takeshima H, Narumiya S, Numa S. Nature 1989;340:230–233. [PubMed: 2474130]
23. Snutch TP, Tomlinson WJ, Leonard JP, Gilbert MM. Neuron 1991;7:45–57. [PubMed: 1648941]
24. Biel M, Ruth P, Bosse E, Hullin R, Stuhmer W, Flockerzi V, Hofmann F. FEBS Lett 1990;269:409–412. [PubMed: 2169433]
25. Lyford GL, Strege PR, Shepard A, Ou Y, Ermilov L, Miller SM, Gibbons SJ, Rae JL, Szurszewski JH, Farrugia G. Am J Physiol Cell Physiol 2002;283:C1001–1008. [PubMed: 12176756]
26. Soldatov NM. Proc Natl Acad Sci U S A 1992;89:4628–4632. [PubMed: 1316612]
27. Hell JW, Westenbroek RE, Warner C, Ahlijanian MK, Prystay W, Gilbert MM, Snutch TP, Catterall WA. J Cell Biol 1993;123:949–962. [PubMed: 8227151]
28. Tang ZZ, Hong X, Wang J, Soong TW. Cell Calcium 2007;41:417–428. [PubMed: 16979758]
29. Restituito S, Cens T, Rousset M, Charnet P. Biophys J 2001;81:89–96. [PubMed: 11423397]
30. Stephens GJ, Page KM, Bogdanov Y, Dolphin AC. J Physiol 2000;525:377–390. [PubMed: 10835041]
31. Hullin R, Singer-Lahat D, Freichel M, Biel M, Dascal N, Hofmann F, Flockerzi V. EMBO J 1992;11:885–890. [PubMed: 1312465]
32. Saada N, Dai B, Echetebu C, Sarna SK, Palade P. Biochem Biophys Res Commun 2003;302:23–28. [PubMed: 12593842]
33. Saada NI, Carrillo ED, Dai B, Wang WZ, Dettbarn C, Sanchez J, Palade P. Cell Calcium 2005;37:301–309. [PubMed: 15755491]
34. Klugbauer N, Marais E, Hofmann F. J Bioenerg Biomembr 2003;35:639–647. [PubMed: 15000524]
35. Sandoval A, Oviedo N, Andrade A, Felix R. FEBS Lett 2004;576:21–26. [PubMed: 15474003]
36. Felix R, Gurnett CA, De WM, Campbell KP. J Neurosci 1997;17:6884–6891. [PubMed: 9278523]
37. Bichet D, Cornet V, Geib S, Carlier E, Volsen S, Hoshi T, Mori Y, De WM. Neuron 2000;25:177–190. [PubMed: 10707982]
38. Gerster U, Neuhuber B, Groschner K, Striessnig J, Flucher BE. J Physiol 1999;517:353–368. [PubMed: 10332087]
39. Takahashi SX, Mittman S, Colecraft HM. Biophys J 2003;84:3007–3021. [PubMed: 12719232]
40. Foell JD, Balijepalli RC, Delisle BP, Yunker AM, Robia SL, Walker JW, McEnery MW, January CT, Kamp TJ. Physiol Genomics 2004;17:183–200. [PubMed: 14762176]
41. Bogdanov Y, Brice NL, Canti C, Page KM, Li M, Volsen SG, Dolphin AC. Eur J Neurosci 2000;12:894–902. [PubMed: 10762319]
42. Chien AJ, Gao T, Perez-Reyes E, Hosey MM. J Biol Chem 1998;273:23590–23597. [PubMed: 9722599]
43. Resh MD. Biochim Biophys Acta 1999;1451:1–16. [PubMed: 10446384]
44. Arien H, Wiser O, Arkin IT, Leonov H, Atlas D. J Biol Chem 2003;278:29231–29239. [PubMed: 12721298]
45. Cho HC, Tsushima RG, Nguyen TT, Guy HR, Backx PH. Biochemistry 2000;39:4649–4657. [PubMed: 10769120]
46. Davis MJ, Hill MA. Physiol Rev 1999;79:387–423. [PubMed: 10221985]
47. Yang Y, Chen X, Margulies K, Jeevanandam V, Pollack P, Bailey BA, Houser SR. J Mol Cell Cardiol 2000;32:973–984. [PubMed: 10888251]

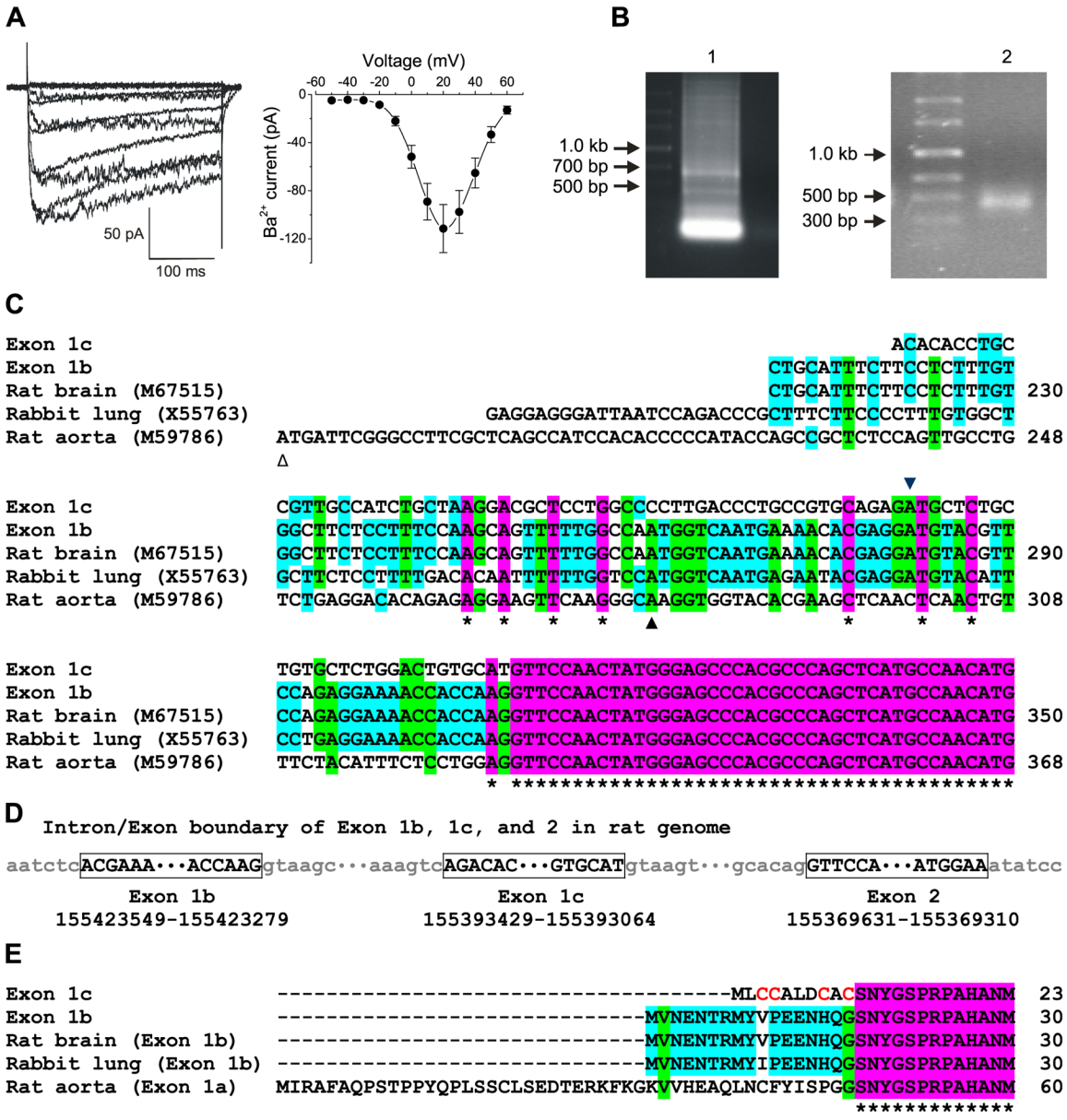

FIGURE 1. Identification of the $Ca_V1.2$ exon 1c in rat cerebral arteries, relative location of exon 1c in the rat genome, and sequence comparison with exons 1a and 1b

A, voltage-dependent Ba^{2+} currents recorded in an isolated myocyte by depolarizing voltage steps (*left panel*) and a mean I-V relationship obtained from 10 cells (*right panel*). *B*, 5′-RACE products from cerebral arteries run in 0.8% agarose gel (*left panel*) with nested PCR products illustrating a band at ~500 bp (*right panel*). *C*, homology of exons 1a, 1b, and 1c compared with $Ca_V1.2$ nucleotide sequences from rat brain (M67515), rabbit lung (X55763), and rat aorta (M59786). The initiation sites of exon 1a, 1b, and 1c are indicated by △, ▲, and ▼, respectively. Part of exon 2 is also illustrated in *purple. D*, schematic diagram depicting the relative locations of exon 1b, 1c, and 2 within the rat genome. *E*, alignment of amino acid sequences encoded by $Ca_V1.2$ exon 1a, 1b, and 1c with part of the exon 2-encoded sequence shown in *purple*. * indicates identical nucleotides or amino acids.

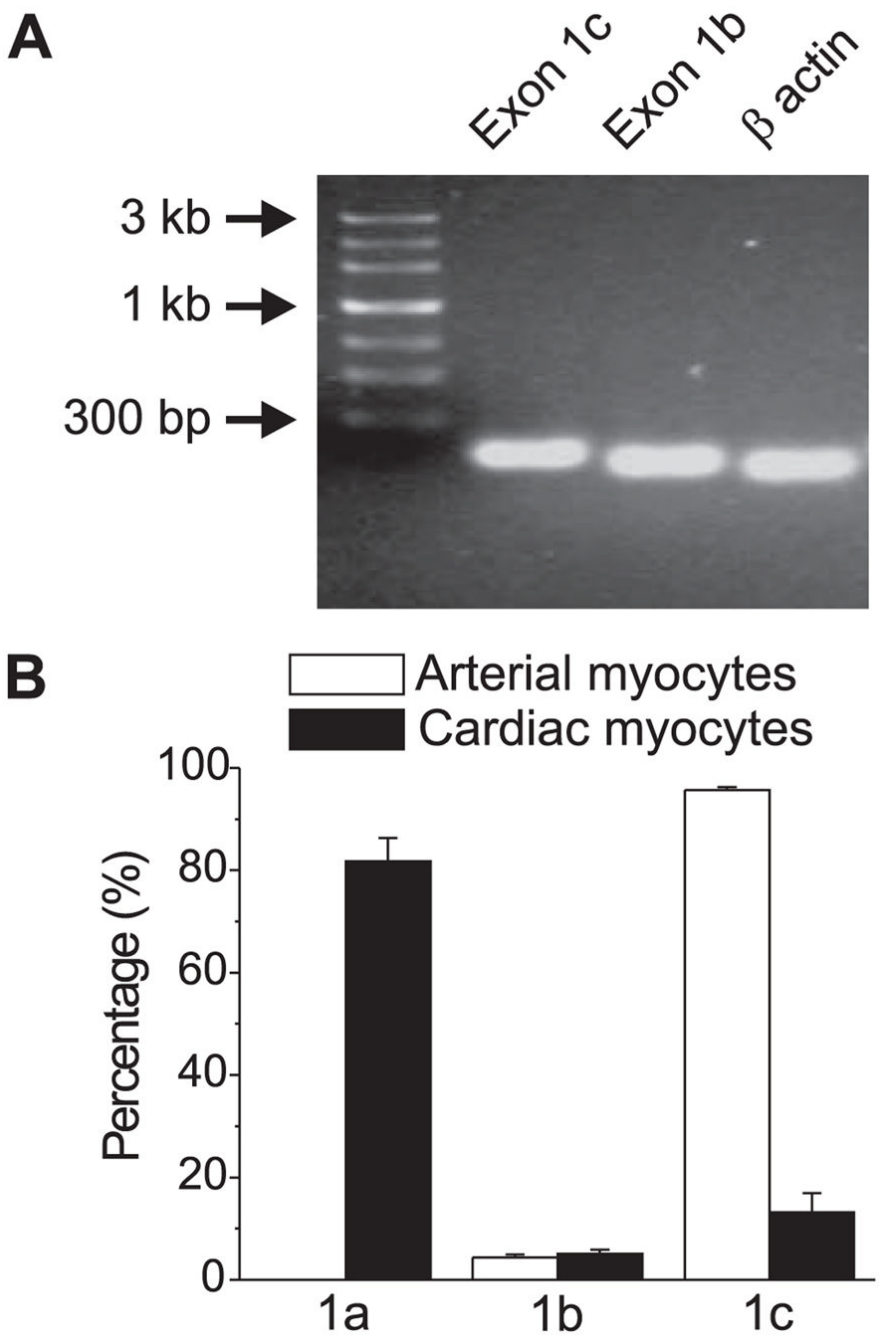

FIGURE 2.

A, RT-PCR revealed the presence of exons 1b and 1c in dissociated cerebral artery myocytes. *β* Actin is shown as a positive control. *B*, real-time PCR indicated the relative percentage of exons 1a, 1b, and 1c message in isolated rat cerebral artery myocytes and cardiac myocytes. Exon 1a was not detected in arterial myocytes.

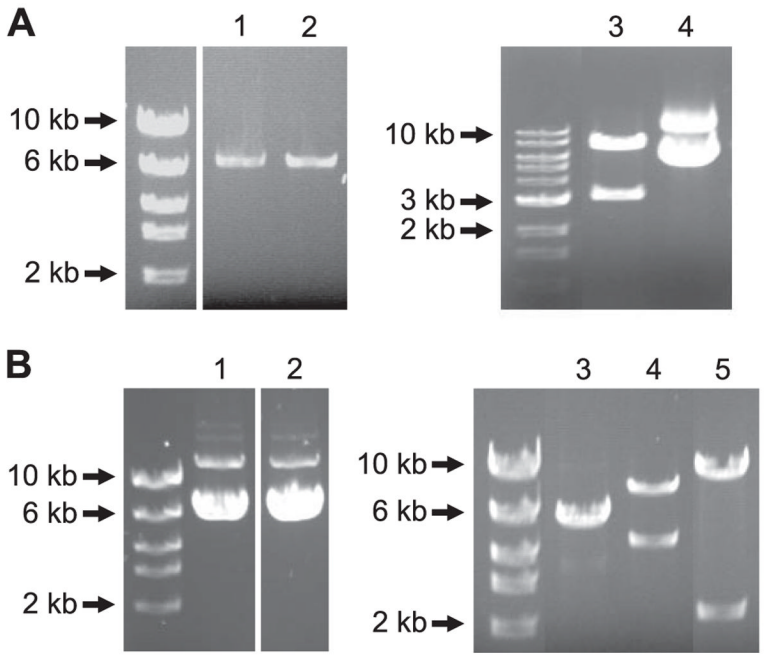

FIGURE 3. Full-length $Ca_V1.2$ cDNAs cloned from rat small cerebral arteries

A, full-length $Ca_V1.2e1b$ and $Ca_V1.2e1c$ were cloned by RT-PCR and sub-cloned into pGEM-T Easy vector. *Lane 1*, $Ca_V1.2e1b$; *lane 2*, $Ca_V1.2e1c$; *lane 3*, $Ca_V1.2e1c$ was released from pGEM-T easy vector by NotI digestion; *lane 4*, pGEM-T easy-$Ca_V1.2e1c$. *B*, $Ca_V1.2e1b$ and $Ca_V1.2e1c$ were subcloned into pIRES-hrGFP II vector, and the orientation direction of $Ca_V1.2$ in the expression vector was revealed by EcoRV digestion. *Lane 1*, pIRES-$Ca_V1.2e1c$-hrGFP II; *lanes 2* and *3*, pIRES-$Ca_V1.2e1b$-hrGFP II; *lane 4*, EcoRV digestion product of pIRES-$Ca_V1.2e1b$(+)-hrGFP II; and *lane 5*, EcoRV digestion product of pIRES-$Ca_V1.2e1b$ (−)-hrGFP II.

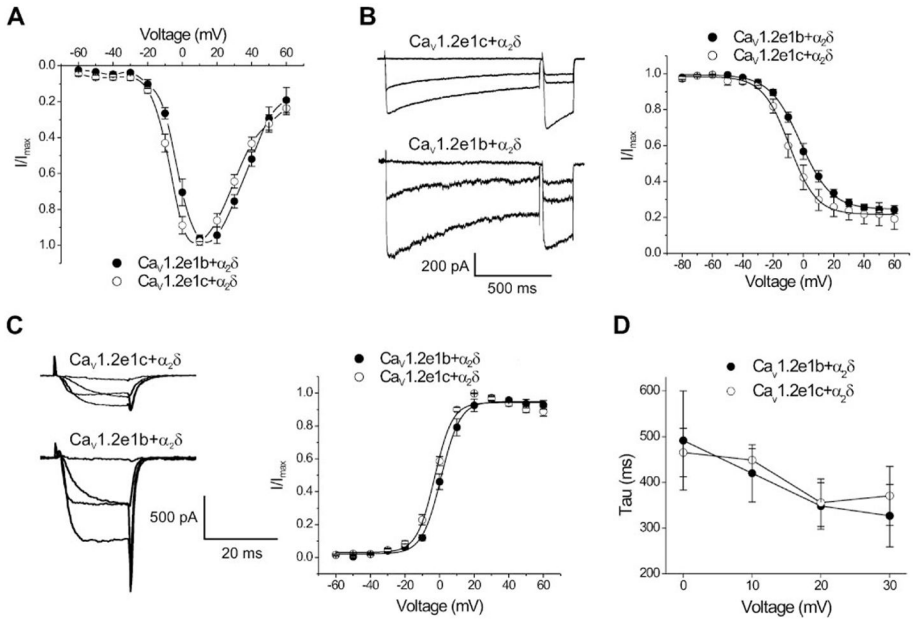

FIGURE 4. Current-voltage (I-V) relationships of $Ca_V1.2e1b$ and $Ca_V1.2e1c$ channels when expressed with auxiliary subunits

Ba_2^+ currents were normalized to facilitate comparison. *A*, I-V relationships of $Ca_V1.2e1b$ and $Ca_V1.2e1c$ when co-expressed with $\alpha_2\delta$. *B*, steady-state inactivation of $Ca_V1.2e1c$ and $Ca_V1.2e1b$ currents when co-expressed with $\alpha_2\delta$. Exemplar current traces of 1-s conditioning depolarizing pulses evoked at −80, +10, and +30 mV followed by 200-ms test pulses to 0 mV (*left panel*). Cell capacitances for original recordings were: $Ca_V1.2e1c + \alpha_2\delta$, 90 pF; $Ca_V1.2e1b + \alpha_2\delta$, 66 pF. Mean steady-state inactivation fit with a Boltzmann function (*right panel*). *C*, voltage-dependent activation of $Ca_V1.2e1c$ and $Ca_V1.2e1b$ currents when co-expressed with $\alpha_2\delta$. Exemplar tail currents evoked by repolarization to −80 mV after depolarizing test pulses to −20, 0, 20, and 40 mV (*left panel*). Cell capacitances for original recordings were: $Ca_V1.2e1c + \alpha_2\delta$, 98 pF; $Ca_V1.2e1b + \alpha_2\delta$, 66 pF. Mean voltage-dependent current activation (*right panel*). *D*, inactivation of $Ca_V1.2e1b/\alpha_2\delta$ and $Ca_V1.2e1c/\alpha_2\delta$ currents were best fit with a single exponential function. Tau was similar for $Ca_V1.2e1b/\alpha_2\delta$ and $Ca_V1.2e1c/\alpha_2\delta$ currents.

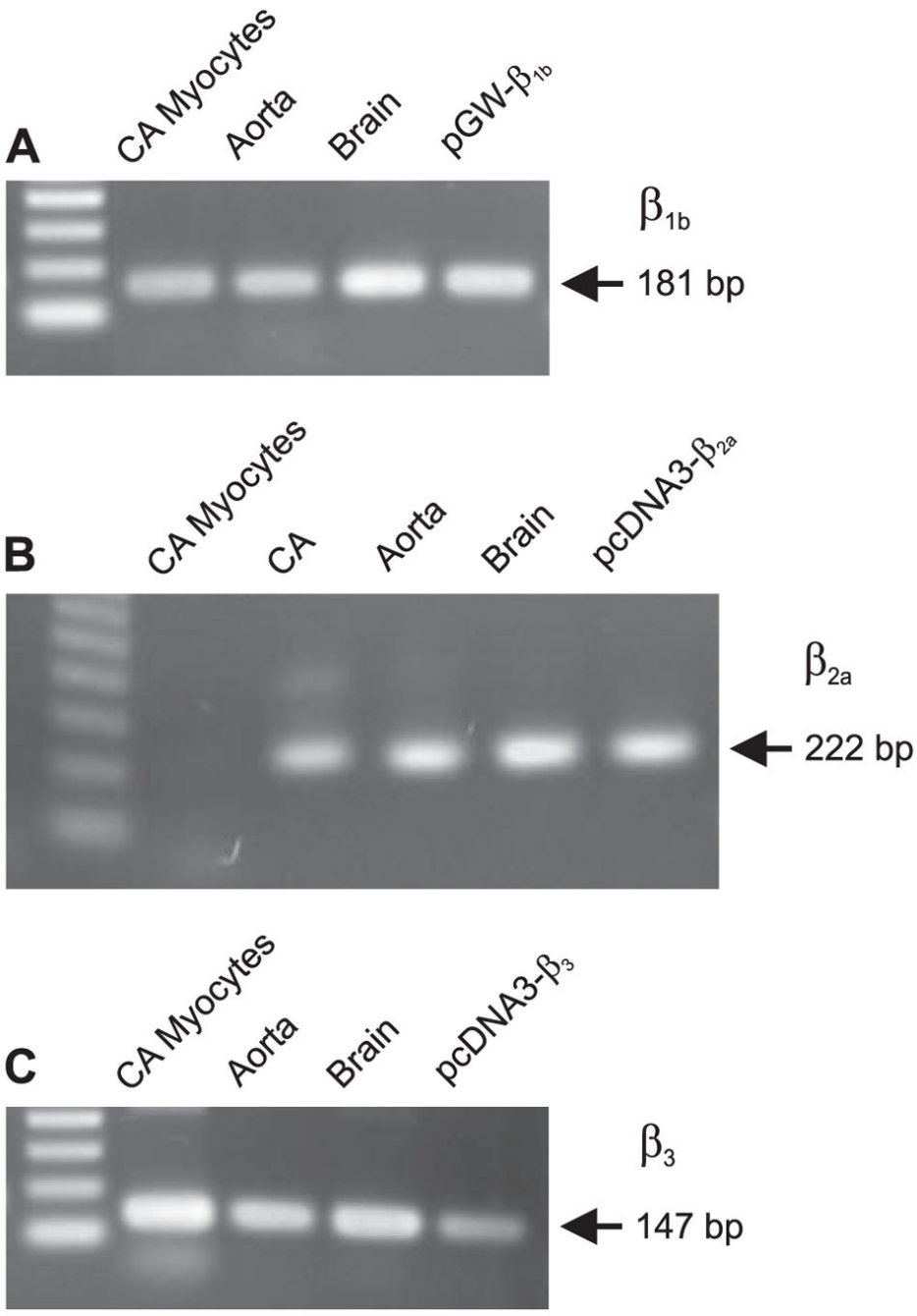

FIGURE 5. RT-PCR of $Ca_V\beta$ subunits expressed in dissociated rat cerebral arterial myocytes
A, β1b subunit. *B*, β_{2a} subunit. *C*, β_3 subunit. *CA* indicates cerebral artery.

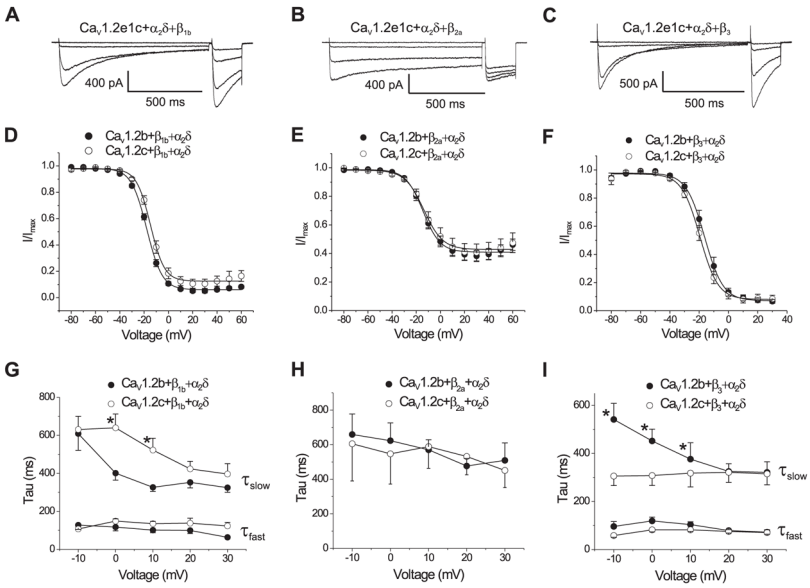

FIGURE 6. Inactivation of $Ca_V1.2e1b/\alpha_2\delta$ and $Ca_V1.2e1c/\alpha_2\delta$ currents when expressed with β_{1b}, β_{2a}, or β_3 subunits

A–C, original recordings of 1-s depolarizing pulses to −80, −20, −10, and 0 mV followed by 200-ms test pulses to 0 mV for each subunit combination indicated. *D–F*, voltage dependence of steady-state inactivation for each subunit combination. *G–I*, voltage dependence of inactivation constants for each combination specified. Inactivation of $Ca_V1.2/\alpha_2\delta/\beta_{1b}$ and $Ca_V1.2/\alpha_2\delta/\beta_3$ currents were best fit with a bi-exponential function representing τ_{fast} and τ_{slow}, whereas $Ca_V1.2/\alpha_2\delta/\beta_{2a}$ current inactivation was best fit with a single exponential. * illustrates $p < 0.05$.

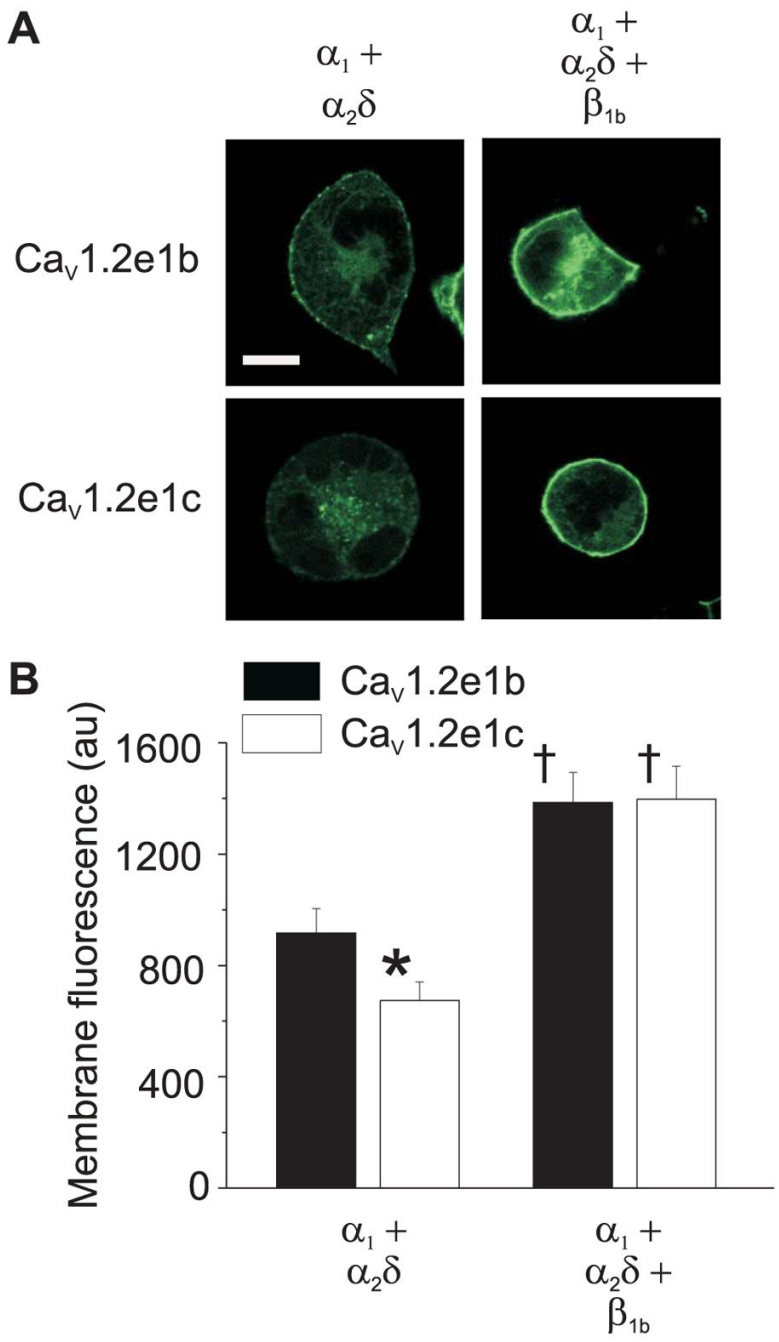

FIGURE 7. Membrane localization of EGFP-tagged $Ca_V1.2e1b$ and $Ca_V1.2e1c$ channels when expressed with $\alpha_2\delta$ or with $\alpha_2\delta + \beta_{1b}$ subunits in HEK 293 cells

A, representative images illustrating cellular fluorescence from EGFP-tagged $Ca_V1.2e1b$ and $Ca_V1.2e1c$ channels when expressed with subunit combinations indicated. *Scale bar*, 10 μm. *B*, mean data illustrating that co-expression of $\alpha_2\delta$ subunits elevated localized membrane fluorescence intensity of $Ca_V1.2e1b$ more than for $Ca_V1.2e1c$, and that co-expression with $\alpha_2\delta + \beta_{1b}$ subunits further increased membrane fluorescence and normalized the difference between $Ca_V1.2e1b/\alpha_2\delta$ and $Ca_V1.2e1c/\alpha_2\delta$. *au* indicates arbitrary units. Number of cells: $Ca_V1.2e1b/\alpha_2\delta$, 18; $Ca_V1.2e1c/\alpha_2\delta$, 16; $Ca_V1.2e1b/\alpha_2\delta/\beta_{1b}$, 17; $Ca_V1.2e1c/\alpha_2\delta/\beta_{1b}$, 20. *

indicates $p < 0.05$ when compared with $Ca_V1.2e1b + \alpha_2\delta$, and †, $p < 0.05$ when compared with the same α_1 subunit + $\alpha_2\delta$.

TABLE 1

Electrophysiological properties of $Ca_V1.2$ channels containing e1b or e1c when expressed alone or co-expressed with auxiliary subunits

Combinations	I-V		Steady-state inactivation			Activation		
	I_{peak} density	*n*	$V_{1/2,inact}$	$\Delta V_{1/2,inact}$ [a]	*n*	$V_{1/2,act}$	$\Delta V_{1/2,act}$ [b]	*n*
	pA/pF		*mV*	*mV*		*mV*	*mV*	
$Ca_V1.2e1c\alpha_1/\alpha_2\delta$	−5.1 + 0.9	6	−9.3 + 1.8		5	−3.0 + 0.8		5
$Ca_V1.2e1c\alpha_1/\beta_{1b}/\alpha_2\delta$	−18.8 + 4.2[c]	9	−14.6 + 0.9[c]	−5.3	8	−7.3 + 1.6	−4.3	7
$Ca_V1.2e1c\alpha_1/\beta_{2a}/\alpha_2\delta$	−19.2 + 3.9[c]	8	−12.9 + 1.0	−3.6	7	−14.9 + 0.7[c]	−12.0	6
$Ca_V1.2e1c\alpha_1/\beta_3/\alpha_2\delta$	−28.6 + 6.8[c]	11	−19.4 + 1.3[c]	−10.1	8	−11.3 + 1.0[c]	−8.4	6
$Ca_V1.2e1b\alpha_1/\alpha_2\delta$	−10.1 + 1.7[d]	5	−1.9 + 2.0[d]		5	1.5 + 1.2[d]		5
$Ca_V1.2e1b\alpha_1/\beta_{1b}/\alpha_2\delta$	−20.9 + 4.7[e]	8	−17.7 + 0.7[e]	−15.8	8	−8.1 + 1.3[e]	−9.6	8
$Ca_V1.2e1b\alpha_1/\beta_{2a}/\alpha_2\delta$	−17.1 + 3.6[e]	10	−14.1 + 1.4[e]	−12.2	9	−15.7 + 1.2[e]	−17.2	9
$Ca_V1.2e1b\alpha_1/\beta_3/\alpha_2\delta$	−27.1 + 5.9[e]	10	−16.2 + 1.7[e]	−14.3	7	−7.5 + 1.1,[de]	−9.0	5

[a] $\Delta V_{1/2,inact}$, β subunit-induced shift in $V_{1/2,inact}$ of corresponding $Ca_V1.2\alpha_1/\alpha_2\delta$ channels.

[b] $\Delta V_{1/2,act}$: β subunit-induced shift in $V_{1/2,act}$ of corresponding $Ca_V1.2\alpha_1/\alpha_2\delta$ channels.

[c] $p < 0.05$ $Ca_V1.2e1c\alpha_1/\beta/\alpha_2\delta$ *versus* $Ca_V1.2e1c\alpha_1/\alpha_2\delta$.

[d] $p < 0.05$ $Ca_V1.2e1b$ *versus* corresponding $Ca_V1.2e1c$.

[e] $p < 0.05$ $Ca_V1.2e1b\alpha_1/\beta/\alpha_2\delta$ *versus* $Ca_V1.2e1b\alpha_1/\alpha_2\delta$.